Atomic Spectroscopy

Article

Direct Sampling GFAAS for Screening Arsenic and Selenium in Fruit Juices

Pavithra Hemachandra,[a] László Bencs,[b] and Zsolt Ajtony [a,*]

[a] Department of Food Science, Wittmann Antal Multidisciplinary Doctoral School of Plant, Animal, and Food Sciences, Albert Kázmér Faculty of Agricultural and Food Sciences, Széchenyi István University, 9200, Mosonmagyaróvár, Lucsonyu. 15-17, Hungary

[b] Photonics Department, Institute for Solid State Physics and Optics, HUN-REN Wigner Research Centre for Physics, P.O. Box 49, 1525 Budapest, Hungary

Received: *May 02, 2026;* ***Revised:*** *July 28, 2026;* ***Accepted:*** *July 28, 2026;* ***Available online:*** *August 01, 2026.*

DOI: 10.46770/AS.2026.0022

ABSTRACT: A digestion-free graphite furnace atomic absorption spectrometry (GFAAS) method was developed for the simultaneous determination of total As and Se in fruit juices using a transversely heated graphite atomizer (THGA) with end-capped pyrolytic graphite tubes fitted with integrated graphite platforms (IGPs). For the analysis, 5 µL of oxidizing reagent (10% (v/v) HNO_3 and 60% (v/v) H_2O_2) with 4 µL of 5 g/L Pd and 5 µL of 0.5 g/L Mg chemical modifier (both applied as nitrates) was directly injected onto the preheated IGP of the THGA (70 ºC) along with 5 µL of juice sample. Optimum pyrolysis and atomization temperatures were 1300°C and 2100°C, respectively. Sensitivity of the method, expressed as the characteristic mass, was 22 pg As and 36 pg Se, in quite good agreement with model calculations (19 pg As and 27 pg Se). LODs were 2.1 µg/L (As) and 2.5 µg/L (Se), well below the European Food Safety Authority (EFSA) limits (20 µg/L). The calibration curves of both As and Se were linear up to 150 µg/L. Method validation with sixteen spiked juice samples yielded average recoveries of 93% for both As and Se. The As and Se contents of all juice samples (apple, grape, orange, peach, and mixed fruit) were below the LOD. A conservative dietary exposure assessment using upper-bound assumptions indicated negligible health risk for both elements. The method provides a rapid, green, and reliable approach for routine screening of As and Se in fruit juices.

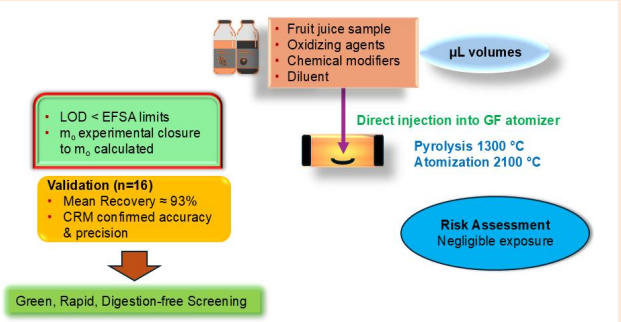

INTRODUCTION

Fruit juice is one of the most popular non-alcoholic beverages consumed worldwide across all age groups. It is valued for its pleasant taste, freshness, and nutritional composition. Fruit juices are recognized worldwide as a rich source of carbohydrate, dietary fiber, macro- and micro-minerals (*e.g.*, Ca, Fe, K, Mg, Mn, Mo, P), vitamins, flavonoids, and phenolic compounds.[1] However, reported mineral contributions to daily intake vary widely across types and brands, highlighting the need for continuous monitoring to ensure compositional consistency and nutritional quality. According to the Agency for Toxic Substances and Disease Registry (2025), arsenic is ranked second and selenium 73rd on the Substance Priority List, reflecting their frequency of occurrence, toxicity, and potential for human exposure.[2] Moreover, the US Food and Drug Administration has initiated Closer to Zero (C2Z) action plan to minimize dietary exposure to toxic elements such as As, Cd, Hg, and Pb in foods commonly consumed by infants and young children.[3]

Arsenic is a metalloid occurring naturally and as a pollutant from anthropogenic activities. It is present in food and water mainly as inorganic species – arsenite (As^{3+}) and arsenate (As^{5+}), which are the most toxic forms – but also are present as thio complexes or oxo anions. Inorganic As (iAs) bound to thio groups of peptides and/or proteins in foods is converted to As^{3+} and As^{5+} during sample preparation and analysis. Therefore, analytical results are generally reported as the sum of arsenite and arsenate. In humans, iAs is efficiently absorbed (45-80%), widely distributed in the body, and able to cross the placental barrier.[4]

Chronic exposure to iAs has been linked to skin cancer, bladder, lung and skin lesions, spontaneous abortion, stillbirth, infant mortality, congenital heart disease, and chronic kidney disease.[4] In most exposure assessments, iAs in drinking water is measured as total As and converted to estimate daily dietary intake.[5] Organic forms of arsenic are rare in terrestrial foods. The most common water-soluble organic As forms are arsenobetaine and arsenosugars, whereas the lipid-soluble forms, arsenolipids, are found in fish, fish products and seaweed.[5, 6]

Selenium is a metalloid occurring naturally in seleniferous soils, but is also released from mining, coal combustion, electronics manufacturing, and agricultural fertilizers enriched with Se compounds.[7] It is an essential trace element involved in antioxidant activity, immune function, reproduction, glucose homeostasis, and thyroid hormone regulation.[8] Despite its essentiality, due to narrow margin between nutritional requirement and toxicity, excessive intake can disrupt key proteins, neurotransmitters, and cellular signaling molecules, potentially leading to neurodegenerative and neuropsychiatric diseases. Inorganic hexavalent selenate is the most common form of Se in drinking water, while selenomethionine is the most common organic form. Both forms have been associated with neurotoxic effects.[8] Safe limits for Se in fruit juices have not yet been established, but inconsistent regulatory limits for drinking water are available. Furthermore, no regulatory framework addresses specific chemical forms of Se. In this study, the EU drinking water directive limit of 20 μg/L was used as the reference.

Organic and inorganic forms of As have been reported in foods across a wide concentration range, from sub-ng/L level to high mg/L levels.[9] Arsenic concentrations in fruit juices and fruit-derived products vary widely, ranging from low μg/L levels to concentrations approaching or exceeding regulatory limits. Studies from Romania[10] and Portugal[11] reported maximum As concentrations of 4.4 μg/L and 13.4 μg/L, whereas concentrations as high as 18.6 μg/L were reported in US fruit juices[12]. Pear concentrates from the USA[13] contained up to 26.2 μg/L As, exceeding the regulatory limit. Fruit-based infant foods reported to contain up to 18 μg/L As and 28 μg/L Se.[14] Elevated As concentrations of up to 26 μg/L have also been reported in Iranian fruit juices.[15] These findings emphasize the importance of continuous monitoring of As and Se in fruit juice and highlight the need for reliable, cost-effective analytical methods suitable for routine screening.

Spectrochemical methods are commonly used to determine trace elements in beverages.[9] Techniques such as flame atomic absorption spectrometry (FAAS), flowing liquid cathode atmospheric pressure glow discharge optical emission spectrometry (FLC-APGD-OES), high-resolution continuum source flame atomic absorption spectrometry (HR-CS-FAAS), graphite furnace atomic absorption spectrometry (GFAAS), inductively coupled plasma mass spectrometry (ICP-MS), inductively coupled plasma optical emission spectrometry (ICP-OES), and X-ray fluorescence spectrometry (XRF) have been used for direct sampling trace element analysis in fruit juices. [12, 16-20] Techniques involving nebulization systems, such as ICP-OES, ICP-MS, and FAAS, generally require sample digestion or pretreatment to prevent nebulizer clogging and matrix interference. Therefore, most studies rely on sample dilution, centrifugation, and filtration steps, prior to analysis, although this is a cumbersome practice for elements present at ultra-trace levels.[12, 18] ICP-MS is a highly sensitive technique, well-suited for multi-element analysis. FAAS and atomic fluorescence spectrometry (AFS), although more economical, are limited by single-element analysis, narrow linear ranges and relatively high detection limits. GFAAS provides excellent sensitivity for trace element quantification and supports direct sampling with minimal sample volume. The analytical capability of multi-element GFAAS has been extended through AA-spectrometers with multiple lamp optics and a beam combiner for hollow cathode or electrodeless discharge lamps, as well as segmented multiarray charge-coupled device (CCD) detectors with 2D optics.[21, 22] HR-CS-AAS further expanded multi-element capabilities through full spectral data acquisition, using an ultra-high pressure xenon arc lamp combined with a high-resolution Echelle double-monochromator and a CCD array-based optics.[22] Although XRF does not demand complex sample preparation, its detection limits are worse (mg/L levels).[23] Meanwhile, FLC-APGD-OES has emerged as a fast, economical, and environmentally friendly direct solution analysis technique. However, its application to fruit juices still requires sample dilution and accurate pH adjustment, limiting its suitability for ultra-trace elemental analysis.[24]

Sample preparation prior to analysis is time-consuming, reagent-demanding, costly, and labor-intensive, while generating significant waste and increasing the risk of analyte loss.[25] It involves wet acid digestion with strong acids and oxidizing agents, like H_2SO_4, $HClO_4$, HNO_3, and H_2O_2, or dry ashing by heating in a muffle furnace or microwave oven, or utilization of extraction and preconcentration techniques to remove organic matter in fruit juice matrix and minimize interference.[17, 26] Although direct sample analysis by GFAAS is more challenging – owing to matrix effects, the need for precise optimization of the furnace heating program, chemical modification for analyte stabilization and matrix removal, and careful control of sample homogeneity and background (BG) absorption – it provides a more sustainable alternative compared to conventional digestion-based instrumental analytical methods.

The present study focuses on developing a direct-sampling GFAAS method for the determination of As and Se in fruit juices, aiming to minimize sample handling, reduce reagent consumption, and enable rapid, environmentally friendly analytical screening. Moreover, simultaneous determination of As and Se within a

single atomization cycle enhances analytical efficiency and precision, while reducing analysis time and resource consumption. To the best of our knowledge, no studies to date have analyzed the As and Se content of fruit juices commercially available on the Hungarian market. Furthermore, although simplified pretreatment techniques such as dilution, centrifugation, and filtration have been practiced in some direct sampling approaches, the application of true direct sample injection – using oxidants, chemical modifiers and diluents directly – into THGA tubes for GFAAS analysis remains scarce, particularly for fruit juice matrices.

EXPERIMENTAL

Instrumentation. The GFAAS measurements were performed using a PerkinElmer Model SIMAA 6000 atomic absorption spectrometer equipped with a transversely heated graphite atomizer (THGA), a longitudinal Zeeman effect background corrector, and a PerkinElmer AS-72 autosampler (PerkinElmer, Überlingen, Germany). End-capped and conventional (standard) THGA tubes with pyrolytically coated integrated graphite platforms (IGPs) were compared for analytical performance. Fruit juice samples, chemical modifiers, oxidizing agents, and diluents were dispensed onto the preheated IGP (70 °C) to minimize sample sputtering and foaming during the drying and pyrolysis steps caused by the high organic matter content. The optimized graphite furnace heating program is presented in Table 1.

Electrodeless discharge lamps for As and Se (PerkinElmer) were operated at currents of 380 mA and 290 mA, respectively. Spectral lines of As 193.7 nm and Se 196.0 nm were selected for the determinations, each with a spectral bandpass of 0.7 nm. Integrated absorbance (A_{int}) signals of As and Se were used for analysis after corrections for non-specific absorption using the Zeeman effect BG corrector. To maintain accurate calibration during extended sample runs, a 50 µg/L As–Se mixed standard was analyzed after every six samples, while the SIMAA 6000 software performed automatic resloping, whenever the sensitivity drift exceeded the permissible tolerance.

Reagents and procedures. Analytical grade 65% (v/v) HNO_3 and Suprapur 30 % (w/w) H_2O_2 (Merck, Darmstadt, Germany) were used to prepare the oxidizing reagent. Dilutions were performed using deionized (ultrapure) water (Milli-Q RG, Millipore, resistance: 18 MΩ cm). As and Se standard solutions were prepared by dilution from a PerkinElmer GFAAS Mixed Standard solution, containing As and Se each at 100 µg/mL. Chemical modifier solutions of various Pd and Mg (nitrate) concentrations were prepared from PerkinElmer modifier solutions, containing 5 g/L Pd and 0.5 g/L Mg (99% purity, Merck). All sample containers and micropipette tips were washed with a 1:1 solution of cc. HNO_3 and then rinsed several times with ultrapure water.

Interference studies were conducted using stock solutions of Merck: KH_2PO_4 (1000±2 mg/L) in water for PO_4^{3-}, NaCl in water (998±2 mg/L) for Cl^-, Na_2SO_4 in water (1002±2 mg/L) for SO_4^{2-}, and iron (1000 mg/L Fe in 5% nitric acid). A 10% (w/v) sugar 'model' solution was prepared by dissolving analytical grade D-(+)-Glucose (Riedel-de Haen, Germany), D-Fructose (Merck), and 0.25% (w/v) citric acid monohydrate (Reanal, Budapest, Hungary) in ultrapure water.

Sample and Standard Preparation. Sixteen fruit juices were purchased from major supermarket chains in Hungary, representing different brands and fruit types, both regular and fortified with minerals and vitamins. The juices were obtained in multiple packaging types, including tetra packs, plastic-, and glass bottles. All samples were stored at 4 °C in their original packaging and thoroughly shaken prior to analysis. A 5 µL aliquot of each sample was directly dispensed onto the IGP along with a 5 µL aliquot of the oxidizing reagent (10% (v/v) HNO_3 and 60% (v/v) H_2O_2), 4 µL of 5 g/L Pd solution, and 5 µL of 0.5 g/L Mg solution.

External calibration standards containing 10, 20, 40, 60, 80, 100, 120, and 150 µg/L of As and Se were prepared by serial dilution of a PerkinElmer Mixed Standard Solution and slightly acidified with 0.2 mL of cc. HNO_3. Blank solutions were prepared following the same procedure, but without the analytes. For standard addition calibration, standards at the same concentrations as for external calibration were prepared by serial dilution of the PerkinElmer Mixed Standard Solution into apple and grape juice samples. For recovery studies, sixteen samples were spiked with a standard solution of 50 µg/L As and Se (corresponding to 0.25 ng dispensed analyte mass), together with the oxidizing reagent at the same concentrations applied for the samples. To study the effect of modifier mass on the sample matrix, Pd and Mg were introduced in three combinations: 5+0.5, 20+0.5, and 20+2.5 µg, each along with 5 µL of an apple juice or blank solution, and 5 µL of oxidizing reagent. The accuracy of the developed method was verified by analysis of a certified reference material (CRM), TMDA-51 Trace Element Fortified Water (National Water Research Institute, Burlington, Ontario, Canada).

To conduct interference studies, a 10 % (w/v) sugar solution was prepared by dissolving 5 g of glucose, 5 g of fructose, and 0.25 g of citric acid in ultrapure water and diluting to 50 mL. A 5 mL of sugar solution was mixed with respective volumes of interferent solutions in a 10 mL conical-bottom laboratory tube and filled up to the mark, diluted with ultrapure water. The effects of Cl^-, PO_4^{3-}, and SO_4^{2-} interferents were assessed at final concentrations of 100, 250, and 500 mg/L, corresponding to injected masses 0.5, 1.25, and 2.5 µg, respectively, while Fe was studied at concentrations of 0.1, 0.5, 1.0, 2.5, and 5.0 mg/L under three Pd–Mg modifier compositions, as described above. A 5 µL aliquot of 10% sugar

Table 1. Optimized graphite furnace heating program for the simultaneous determination of As and Se in fruit juice samples

Step	Temperature (°C)	Ramp time (s)	Hold time (s)	Internal Ar flow rate (mL/min)
Drying 1	110	2	30	250
Drying 2	130	10	30	250
Pyrolysis 1	400	10	20	250
Pyrolysis 2	1300	10	20	250
Atomization	2100	0	5	0
Cleaning	2450	1	3	250

solution/ultra-pure water with interferents was injected together with 5 µL of the optimized oxidizing reagent, spiked with 50 µg/L each of As and Se. Potential memory effects were assessed by measuring reagent blanks and unloaded graphite tubes immediately after measuring the highest-spiked concentrations in fruit juice samples.

Statistical and evaluation methods. The evaluation of measurement data (duplicate for each sample) was based on descriptive statistics, including calculation of arithmetic mean, standard deviation (SD), and relative standard deviation (RSD). Data processing and graphical evaluation were performed using Microsoft Excel. The effect of inorganic interferents was evaluated by comparing the integrated absorbance obtained for interferent-containing sugar solutions with that of the corresponding aqueous (acidic) standard:

$$Recovery\ (\%) = \frac{A_{smx}}{A_{std}} \times 100 \qquad (1)$$

where A_{smx}: integrated absorbance measured for the 10% sugar matrix solution containing the interferent, and A_{std}: integrated absorbance measured for the ultrapure water containing the same amount of interferent.

The linearity of the calibration was presented as the coefficient of determination (R^2) from least-squares linear fits to calibration points. Error bars in the graphs represent the measurement SDs. The limit of detection (LOD) values were obtained as three times the SD from eleven consecutive blank measurements divided by the calibration slope (S_c): LOD = 3SD/S_c. The characteristic mass (m_o) representing GFAAS sensitivity, was determined as the analyte mass yielding an integrated absorbance of 0.0044 s.[27-29] Its experimental value ($m_{o,exp}$) was evaluated using the following formula:

$$m_{o,exp} = \frac{0.0044\ c\ v}{A_{std} - A_{bl}} \qquad (2)$$

where c is the analyte concentration of a calibration standard (µg/L), v is the injected solution volume (µL), A_{std} is the integrated absorbance (s) measured for the calibration standard, A_{bl} is the integrated absorbance (s) for a corresponding blank.

The theoretical characteristic mass ($m_{o\ cal}$) of As and Se was calculated by means of previous model studies[30, 31] and the diffusional residence time model for free atoms in end-capped THGA tubes, proposed by Hadgu et al.[32] The temperature-dependent parameters in the formula of $m_{o\ cal}$ were calculated for the atomization temperature (T_{at}) optimized for each analyte.[31,33,34] The software (THECHARMAS) for theoretical m_o calculations, previously written in Borland Turbo Pascal 6.0,[33] was modified for the current calculus.

Percent recovery for spiked fruit juice sample analysis was calculated as follows:

$$Recovery\ (\%) = \frac{C_{spiked} - C_{original}}{C_{added}} \times 100 \qquad (3)$$

where C_{spiked} is the concentration of the analyte measured in the spiked sample, $C_{original}$ is the concentration of the analyte in the corresponding unspiked sample, and C_{added} is the concentration of the analyte added during the spike experiment.

Linear regression analysis was performed using Minitab (version 22.2.1.0) to assess the relationship between estimated dry matrix residue and analyte recovery. The R^2 and the p-value obtained from ANOVA were used to assess the strength and statistical significance of the regression ($p<0.05$).

The environmental sustainability of the developed method was assessed using AGREE (Analytical GREEnness) software (version 0.4, 2020), which is based on the twelve principles of green analytical chemistry.[35] The assessment considered sample preparation, sample volume and number, analytical waste generation, instrument configuration, degree of automation, energy consumption, sample output per analytical cycle, and type and hazards of the reagents used. The AGREE software integrates these parameters into a single numerical score ranging from 0 (least environmentally friendly) to 1 (most environmentally friendly) and displays the results as a circular pictogram, where each of the twelve principles is color-coded from red (poor compliance) to dark green (excellent compliance).

RESULTS AND DISCUSSION

Optimization of graphite furnace heating program. Two-step drying and pyrolysis stages were applied in the graphite furnace

heating program to ensure complete and controlled removal of solvents and organic compounds from fruit juice samples. The gradual temperature increases during the drying steps minimized sample sputtering and foaming. The two-step pyrolysis allowed progressive decomposition of the organic matrix, thereby reducing carbon residue formation and preventing analyte loss prior to atomization. A similar strategy has been used to analyze trace metals in wine samples.[36] Identifying optimal compromise values for pyrolysis temperature (T_{pyr}) and T_{at} is crucial in simultaneous GFAAS analysis. The compromise T_{pyr} is determined by the most volatile element, while the most refractory element determines the compromise, T_{at}. Regarding the current analytical task, As is more volatile in the graphite furnace than Se.

Figure 1 shows the pyrolysis and atomization curves of 1 ng of each As and Se in an acidic standard using the lowest modifier mass (5 µg Pd + 0.5 µg Mg) in conventional and end-capped THGA tubes. Both analytes showed limited thermal stability during pyrolysis and sharp signal loss above 1200 °C. Increasing the amount of Pd to 20 µg (Fig. 2) enhanced the thermal stability of both analytes, likely due to the formation of intermetallic Pd–As and Pd–Se phases[37] or intercalation compounds, [38, 39] which prevent early-stage vaporization during pyrolysis. Addition of a larger amount of Mg (e.g., 2.5 µg) with 20 µg Pd (Fig. 3) further increases thermal stabilization by promoting matrix decomposition, assisted by MgO ashing aid residues that delay analyte volatilization. As a result, both analytes withstand higher T_{pyr} (1300 °C), while delivering significantly enhanced atomization peaks at 2100 °C. With all modifier combinations studied, end-capped THGA tubes consistently produced higher A_{int} signals than conventional THGAs, due to the longer residence time of analyte atoms and reduced loss through the tube ends. The simultaneous determination of As, Cd, Pb, and Se in water samples was performed using end-capped THGAs and a Pd-Mg modifier (up to 16+10 µg).[36] The compromise T_{pyr} and T_{at} were 800 °C and 2200 °C, respectively. Their lower optimal T_{pyr} value was largely influenced by Cd, which volatilized at lower temperatures than the other analytes. Despite differences in pyrolysis behavior, the optimal T_{at} in both studies was similar, confirming that end-capped THGA tubes provide reproducible and stable conditions for As and Se atomization. Vinter *et al.*[40] determined Se in deionized water and acetic acid leachates of hazardous waste using GFAAS, without and with chemical modifiers (5 µg Pd + 2.5 µg Mg). Without modifiers, the optimal T_{pyr} and T_{at} were 300 °C and 2100 °C, respectively. With modifiers, T_{pyr} increased to 1050 °C, while T_{at} remained unchanged, demonstrating the stabilizing effect of the modifiers and allowing higher T_{pyr}, thus more efficient matrix removal. Modifiers also improved the atomization transient to a single Gaussian peak, whereas without modifiers, double peaks were observed due to partial vaporization and atomization of Se at lower temperatures. Dakuzaku *et al.*[41] directly determined As in sugar solutions by GFAAS and evaluated Ni, Pd, and Pd+Mg modifiers to optimize

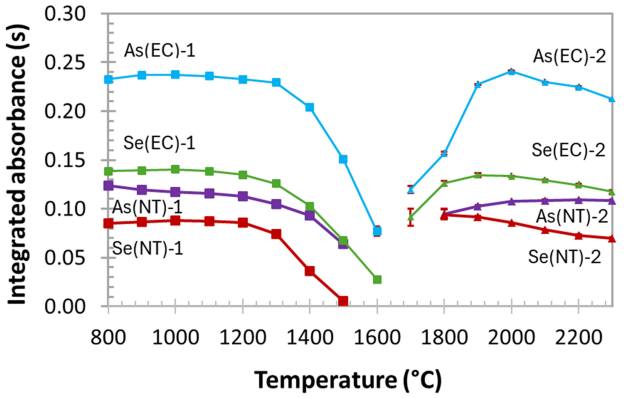

Fig. 1 Pyrolysis (1) and atomization (2) curves 1.0 ng As and 1.0 ng Se with 5 µg Pd+0.5 µg Mg using conventional (NT) and end-capped (EC) THGA tubes.

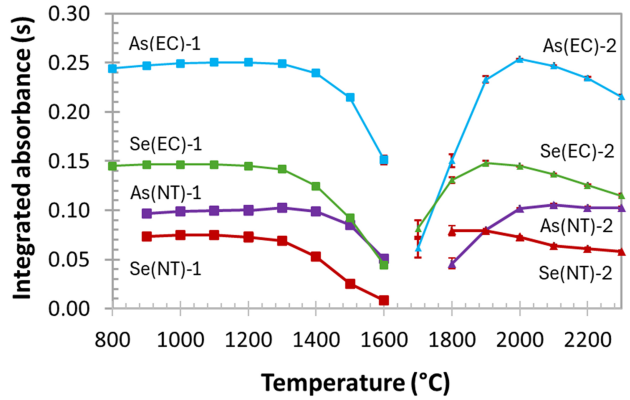

Fig. 2 Pyrolysis (1) and atomization (2) curves for 1.0 ng As and 1.0 ng Se with 20 µg Pd+0.5 µg Mg using conventional (NT) and end-capped (EC) THGA tubes.

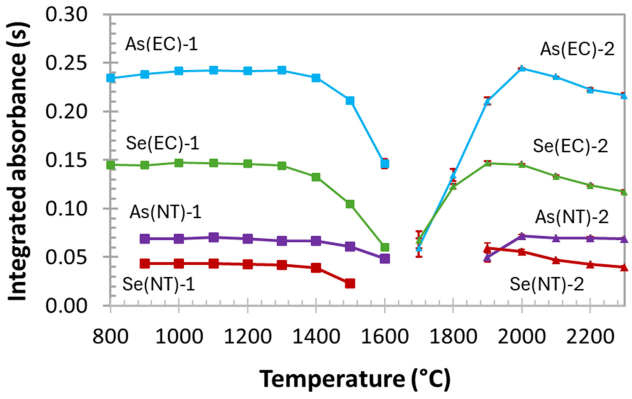

Fig. 3 Pyrolysis (1) and atomization (2) curves for 1.0 ng As and 1.0 ng Se with 20 µg Pd+2.5 µg Mg using conventional (NT) and end-capped (EC) THGA tubes.

Table 2. Effect of sample volume and Pd–Mg modifier composition on the recovery of 0.25 ng of As and Se spikes in an apple juice sample

Sample volume (µL)	Recovery ±SD (%) with different amount of the Pd–Mg modifier composition					
	5 µg Pd + 0.5 µg Mg		20 µg Pd + 0.5 µg Mg		20 µg Pd + 2.5 µg Mg	
	As	Se	As	Se	As	Se
3	94.0±2.2	99.5±1.7	103.1±2.5	103.7±1.0	103.4±2.1	102.7±3.5
5	76.4±2.1	90.8±4.8	94.1±1.2	93.2±2.1	99.9±2.4	100.5±3.1
10	61.4±1.8	72.7±1.1	74.1±2.2	83.6±1.2	74.4±1.6	83.7±3.7
15	47.9±0.7	56.8±2.8	57.0±2.6	63.0±0.6	63.2±2.3	65.6±2.6
20	29.4±0.3	34.8±2.4	49.5±3.1	53.1±1.4	54.8±3.9	56.0±1.5

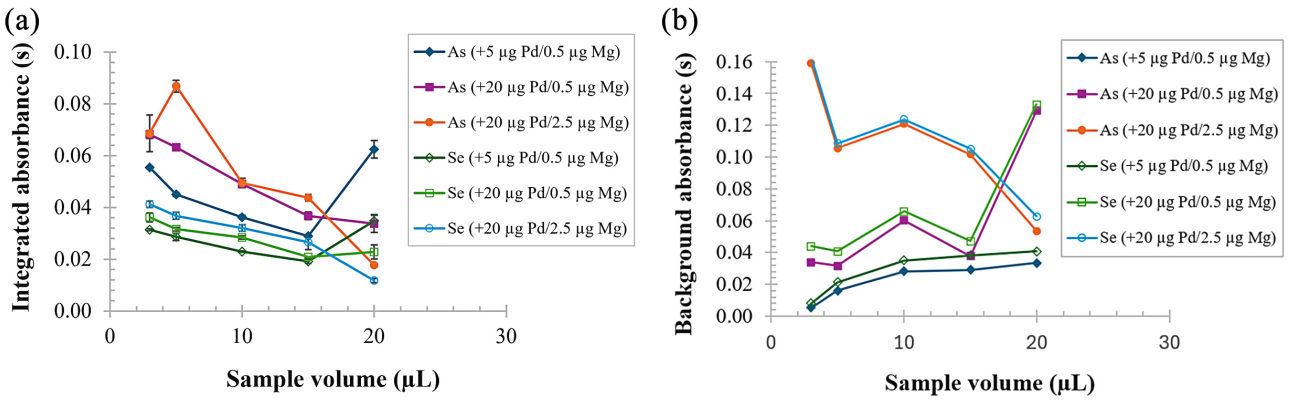

Fig. 4 Effect of sample volume and Pd–Mg modifier composition on the integrated absorbance (a) and background absorbance (b) of 0.25 ng of each As and Se spikes in apple juice.

the pyrolysis and atomization conditions. Ni stabilized As up to 1600 °C, whereas Pd and Pd+Mg showed optimum pyrolysis at 1400 °C. Finally, Pd was selected for analysis, because of the highest sensitivity, narrower absorbance peak, and more effective background suppression. A two-step pyrolysis was also employed to reduce BG absorption arising from decomposition of sugar matrix, similar to the approach used in the present study.

Study on sample volume and memory effect. The influence of sample volume (3–20 µL) and modifier composition on analyte signal recovery was evaluated using apple juice spiked with 0.25 ng of As and Se. For all modifier combinations, the recovery decreased progressively with increasing sample volume (Table 2), likely owing to the increased matrix load. Based on the labeled sugar content of the assessed apple juice (7.8%), the injected sample volumes correspond to estimated dry matrix residues of approximately 0.23 mg at 3 µL, 0.39 mg at 5 µL, 0.78 mg at 10 µL, 1.17 mg at 15 µL, and 1.56 mg at 20 µL. At higher matrix loads, incomplete matrix decomposition or partial analyte loss during pyrolysis is likely. Recoveries close to 100% were achieved at both 3 and 5 µL sample volumes. A sample volume of 5 µL was selected as optimal, providing sufficient analyte mass on the graphite platform, thereby improving method robustness and analytical sensitivity.

The effect of sample volume on the atomization transients (Figs. S1 and S2) was evaluated by observing the appearance time (t_{app}) and peak time of As and Se (Table S1). As the sample volume increased from 3 to 20 µL, the t_{app} of both elements increased only marginally (As: 1.04 to 1.2 s; Se: 0.75 to 0.84 s). Peak time also varied slightly for both analytes; with no systematic shift observed across the assessed sample volume range. These results indicate that sample volume has a small influence on the atomization timing. However, a progressive decrease in analyte recovery with increasing sample volume suggests that greater matrix load led to incomplete matrix decomposition or partial analyte loss during pyrolysis, rather than substantially altering atomization behavior. Taken together with the recovery studies, these results support 5 µL as the optimum sample volume for subsequent analysis.

No measurable memory effects were observed under optimized conditions. Reagent blanks and unloaded graphite tube measurements performed immediately after analysis of spiked fruit juice samples showed only background-level signals, while no carbonaceous residues on the graphite platform were found. This indicates negligible carry-over between analytical cycles.

Effect of chemical modifier on analytes and matrix. Chemical modifiers are widely used in GFAAS analysis to thermally stabilize volatile analytes, preventing premature vaporization prior to atomization and minimizing matrix effects.[42] The influence of modifier composition on the analyte signal is visualized in Fig. 4a. At each sample volume assessed, increasing Pd–Mg modifier masses generally increased the A_{int} signal for both As and Se,

Table 3. Recoveries for 0.25 ng of As and Se obtained at different Pd–Mg modifier compositions in the presence of various chloride, phosphate, and sulphate masses (0.5, 1.25, and 2.5 µg)

Chemical Modifier	Interferent	Recovery ±SD (%) at increasing interferent amount (µg)					
		0.5		1.25		2.5	
		As	Se	As	Se	As	Se
5 µg Pd + 0.5 µg Mg	Chloride	73.5±0.7	90.8±1.2	64.5±0.7	80.7±1.0	66.2±1.1	76.8±0.9
	Phosphate	73.4±1.1	64.8±1.3	59.8±1.2	65.7±0.9	44.2±1.2	63.5±1.5
	Sulfate	94.4±2.1	65.3±1.7	87.6±3.9	63.4±1.3	78.1±1.4	54.7±0.8
20 µg Pd + 0.5 µg Mg	Chloride	94.0±5.0	96.3±1.3	82.7±1.1	90.3±3.4	77.2±2.6	90.9±4.0
	Phosphate	77.3±3.1	92.0±1.3	62.8±0.5	87.1±1.2	54.9±0.9	82.1±1.8
	Sulfate	84.4±0.7	65.3±1.7	88.2±0.9	63.4±1.3	86.8±2.1	54.7±0.8
20 µg Pd + 2.5 µg Mg	Chloride	95.7±1.0	99.9±1.1	93.2±0.9	92.6±2.5	94.6±0.7	94.4±2.8
	Phosphate	89.7±2.8	95.1±2.9	75.4±3.3	95.0±2.5	69±1.4	90.6±1.3
	Sulfate	103.8±0.8	93.3±2.1	101.8±1.0	89.7±1.6	102.7±1.5	88.4±2.0

indicating improved thermal stabilization and reduced analyte loss during pyrolysis. The beneficial effect became more pronounced at larger sample volumes, where increased matrix loading would otherwise suppress the analytical signal. The highest analyte signal was obtained with the 20 µg Pd + 2.5 µg Mg at a 5 µL sample volume. Among the assessed modifier compositions, 20 µg Pd +2.5 µg Mg consistently provided recoveries closest to 100% for both analytes. Increasing the Pd amount to 20 µg (while keeping Mg at 0.5 µg), markedly improved As recovery from 76.4% to 94.1% at the selected sample volume of 5 µL. Further increasing the Mg mass from 0.5 µg to 2.5 µg enhanced the recovery of both analytes to near-quantitative levels. The lowest modifier mass (5 µg Pd + 0.5 µg Mg) yielded relatively low recovery for As and Se (Table 2), indicating partial analyte loss in the THGA during pyrolysis. The beneficial effect of chemical modification becomes increasingly important at higher matrix loads. Overall, this modifier composition minimized analyte loss, while promoting oxidation and removal of the organic matrix constituents. Accordingly, 20 µg Pd + 2.5 µg Mg was selected as the optimal modifier composition for subsequent measurements. The variability of background absorbance with modifier composition and sample volume is presented in Fig. 4b. Increasing the modifier mass generally increased the background signal; however, the background absorbance remained within the correction capability of the Zeeman effect BG correction system.

Effect of interferents. In complex matrices, such as fruit juices, inorganic compounds – particularly halides (*e.g.*, chlorides), sulfates, and phosphates – can significantly influence the atomization of target elements.[43] During graphite furnace heating cycle, volatile halide compounds such as $AsCl_3$, $SeCl_2$, and $SeCl_4$ can form in the gas phase, resulting premature vaporization and analyte loss. In contrast, thermally stable phosphate salts can cause incomplete atomization and vaporization loss in molecular form from THGAs. In particular, PO has intense bands in the far UV (*e.g.*, at 193.3 and 197.1 nm),[44] which may cause structured BG absorption at the analytical lines studied. Molecular bands of PO and NO, formed from phosphate- and nitrate-containing matrix components during pyrolysis and atomization were reported to produce broadband absorption near the Se resonant line (196.026 nm).[40, 45] These interferents may produce variable BG absorption and reduce sensitivity for Se through under- and overcompensation errors in GFAAS systems utilizing conventional continuum-source BG correction.[46] Consequently, chemical modifiers play a crucial role in tackling these interferences. The combined use of Pd and Mg modifiers enhances analyte stabilization by controlling the thermal decomposition of organic and inorganic matrix constituents and minimizing analyte loss.

The effects of chloride, phosphate, and sulphate on analyte recovery under different modifier compositions are summarized in Table 3. Among the evaluated interferents, phosphate showed the strongest suppressive effect on analyte recovery. Under optimized modifier amounts (20 µg Pd +2.5 µg Mg), the recovery of As decreased from 89.7% to 69.0% when the introduced phosphate mass increased from 0.5 to 2.5 µg. In contrast, chloride produced only moderate interference, whereas sulfate showed the least interference. Increasing Pd and Mg masses substantially improved analyte recovery in the presence of all investigated interferents. However, recoveries decreased gradually with increasing interferent mass, indicating that although the optimized modifier effectively reduced interference effects, its efficiency was partially limited at the highest interferent masses (*i.e.*, 2.5 µg). Overall, 20 µg Pd +2.5 µg Mg modifier composition provided the highest recovery under all assessed interference conditions, confirming that the optimized mass of Pd–Mg modifier effectively suppressed the matrix-induced interferences studied and improved analyte stabilization during direct-sampling GFAAS analysis of fruit juices.

Cabon and Le Bihan reported that Pd was less effective in stabilizing Se in the presence of sulphate in seawater than in chloride media, resulting in lower atomization efficiency, because Pd provided only partial stabilization of Se in sulfate-containing matrices.[47] This observation is consistent with the present results: increasing Pd mass alone does not fully eliminate sulphate-induced suppression of Se, until the Mg mass is increased to 2.5 µg,

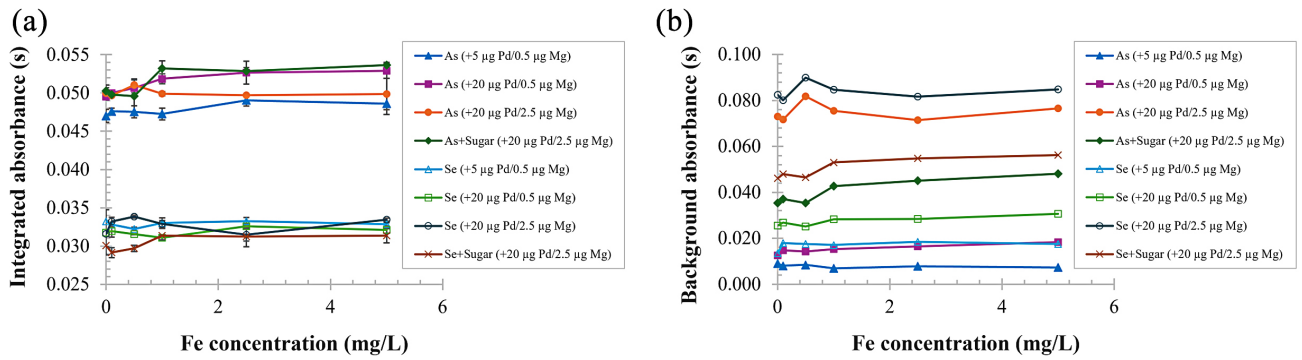

Fig. 5 Integrated absorbance (a) and background absorbance (b) of 0.25 ng of each As and Se at different Pd–Mg modifier compositions and iron interferent concentrations.

Table 4. Analytical performance data with various amounts of the chemical modifier

Analyte	Pd + Mg Mass (µg)	Slope (s L/µg)	R^2	Absolute LOD (pg)	$m_{o\,exp}$ (pg)
As	5 + 0.5	0.00093	0.9987	38.8	47
	20 + 0.5	0.00099	0.9995	36.3	44
	20 + 2.5	0.00100	0.9998	10.5	22
Se	5 + 0.5	0.00078	0.9990	46.4	57
	20 + 0.5	0.00072	0.9988	50.0	61
	20 + 2.5	0.00061	0.9997	12.5	36

Abbreviations: R^2 - coefficient of determination for linear fitting, $m_{o\,exp}$ - experimental characteristic mass, Absolute LOD - limit of detection for sample volumes of 5 µL with Pd–Mg masses of 20+2.5 µg and sample volumes of 10 µL with Pd–Mg masses of 5+3 µg, and 20+0.5 µg.

indicating that Mg complements the stabilizing effect. Cabon and Le Bihan also suggested that Mg contributes substantially to stabilizing Se in GFAAS by minimizing the volatilization of molecular Se species.[47] Pretreated Pd effectively reduced the chloride-induced interference by increasing T_{pyr} to 1200 ºC, thereby enabling removal of the chloride matrix before atomization and maintaining A_{int} within an ≈10% variation.[47] Similarly, chloride produced only moderate interference in the present study, with acceptable recoveries obtained under all modifier compositions except at the lowest Pd mass (5 µg) combined with the highest chloride mass (2.5 µg).

According to the NIST Atomic Spectra Database[49], several Fe I (195.570 nm, 195.784 nm, 195.857 nm, 195.861 nm, 195. 873 nm, 196.014 nm, 196.062 nm, 196.104 nm, 196.124 nm, 196.202 nm, 196, 211 nm), Ni I (196.387 nm), and Co I (195.422 nm, 195.517 nm, 195.855 nm, 196.159 nm) lines lie close to the Se resonant line (196.026 nm), while for the analytical line of As (at 193.36 nm), the Co I (193.593 nm), and Fe I (at 193.388 nm, 193.661 nm, and 194.001 nm) may cause spectral interferences. Although the Co and Ni content of fruit juices is low (*e.g.*, <0.2–38 and <0.27-114 µg/L, respectively), the Fe content may vary in the range from 0.16 to 3.7 mg/L.[50] Since Fe has the potential to contribute to the spectral background in the vicinity of As and Se analytical lines, it was investigated in the current study.

The A_{int} signal of both As and Se remained essentially constant over the studied Fe concentration range (Fig. 5a), indicating that iron caused no measurable interference under the optimized analytical conditions. Similar behavior was observed in both matrix-free (acidic) and sugar-containing standards. Only a negligible change in background absorbance was observed over the assessed Fe concentration range (Fig. 5b); associated with the amounts of Pd–Mg modifier injected onto the graphite platform rather than with the Fe concentration. These finding are in line with the lower susceptibility of GFAAS systems utilizing Zeeman BG correction to spectral interferences, compared to conventional continuum-source BG correction (*e.g.*, D_2-lamp).[46]

Calibration and analytical performance. The effect of the chemical modifier mass on the slope and linearity of external calibration, method sensitivity ($m_{o\,exp}$), and LODs for As and Se were assessed (Table 4). For both analytes, the calibration curves showed excellent linearity (R^2 > 0.999). The upper limit of the linear calibration range was 150 µg/L for both As and Se, which is a broader dynamic range than that observed in an earlier study.[36] For As, calibration slopes increased slightly with increasing modifier mass, from 0.00093 to 0.00100 s L/µg, improving the LOD. The 20 µg Pd + 2.5 µg Mg modifier dose yielded the highest R^2 values and slopes for both analytes, along with the lowest $m_{o\,exp}$ and LOD values, indicating the best overall sensitivity. Se showed slightly lower slopes, higher LODs and higher $m_{o\,exp}$ compared to As.

To verify the trueness of external calibration, standard addition was performed directly on the IGP by sequentially dispensing undiluted fruit juice (apple or grape) and defined volumes of As and

Table 5. Comparison of external (matrix-free) and standard addition calibration

Analyte	Matrix/calibration	Slope (s L/µg)	Slope bias (%)	R^2
	matrix-free/external	0.00123	-	0.9959
As	apple juice/std. add.	0.00128	4.5	0.9983
	grape juice/std. add.	0.00130	5.7	0.9943
	matrix-free/external	0.00066	-	0.9946
Se	apple juice/std. add.	0.00065	-1.1	0.9919
	grape juice/std. add.	0.00061	-7.2	0.9956

Note: The *slope bias* was calculated using the slope of external (matrix-free) calibration as a reference for each analyte.

Table 6. Experimental ($m_{o\,exp}$) and theoretical ($m_{o\,cal}$) characteristic masses for As and Se obtained in the present study for end-capped THGAs and the manufacturer's reference ($m_{o\,exp\,PE}$) data for standard THGAs

Analyte	$m_{o\,exp}$ (pg)	$m_{o\,cal}$ (pg)	$m_{o\,exp\,PE}$ (pg)
As	22	19	40
Se	36	27	45

Se standard solutions, with added concentrations up to 150 µg/L. The calibration slopes obtained by standard addition were comparable to those from external matrix-free calibration (Table 5). For As, the slopes obtained in apple and grape juice were 104.5% and 105.7% of the external calibration slope, respectively (Table 5). For Se, the corresponding values were 98.9% and 92.8%, respectively. These results indicate that matrix effects are minor (slope bias for As: +4.5 to +5.7%, for Se: -7.2 to -1.1%) and that external (matrix-free) calibration can be applied to the determination of As and Se in fruit juice samples under optimized analytical conditions.

Increasing the amount of Mg from 0.5 to 2.5 µg substantially improved the absolute LOD (for a 5-10 µL sample) from 38.8 to 10.5 pg for As and from 46.4 to 12.5 pg for Se. Importantly, LODs obtained with the optimal modifier mass (20 µg Pd + 2.5 µg Mg) – 2.1 µg/L (10.5 pg) for As and 2.5 µg/L (12.5 pg) for Se – were well below the maximum allowable concentration for iAs in fruit juice (20 µg/L; European Food Safety Authority – EFSA), for total As in drinking water (10 µg/L; European Commission), and for Se in drinking water (20 µg/L; EFSA).[5, 51]

The LOD values obtained in this study are consistent with those from former GFAAS studies using direct sample introduction. A LOD of 5 µg/L and $m_{o,\,exp}$ of 24 pg was reported for As in wine analysis using Pd+Mg (5+3 µg) and end-capped THGAs.[36] A four times larger modifier mass slightly improved the LOD and $m_{o\,exp}$ to 3.9 µg/L and 20 pg, respectively. A study on natural and drinking water[52] resulted in better LODs for As and Se (1.9 and 1.3 µg/L, respectively) using 16 µg Pd + 10 µg Mg, consistent with the lower matrix complexity of water compared to fruit juice. Michon *et al.*[53] obtained LODs below 1 µg/L for iAs in water using high-intensity UltrAA-lamps, demonstrating that enhanced primary light source intensity can significantly reduce baseline noise in AAS. Earlier, Bezúr[54] showed that boosted hollow cathode lamps can increase the sensitivity of As and Se determination by 30%. More recently, Vinter *et al.*[40] reported a LOD of 5.2 µg/L for Se in GFAAS analysis of hazardous waste leachates using Pd–Mg modifiers in end-capped THGA tubes – approximately twice the sensitivity of the modifier-free method (LOD: 9.8 µg/L). Although some GFAAS studies report significantly lower LODs than the present investigation, these typically involve preconcentration or extraction techniques.[53]

Comparison of experimental and theoretical sensitivity. Under optimized conditions, including the best-performing modifier mass, the $m_{o,\,exp}$ values for As and Se are 22 pg and 36 pg, respectively (Table 6), indicating ≈1.6-fold higher sensitivity for As than for Se. In a previous study, $m_{o\,exp}$ values of 35 pg As and 46 pg Se using standard THGA tubes was reported.[33] Compared to these data, the current $m_{o\,exp}$ values acquired with end-capped THGAs represent sensitivity increases of about 1.6- and 1.3-fold for As and Se, respectively. The end-capped design markedly reduces axial diffusion loss and increases the residence time of free atoms in the optical path, systematically lowering m_o. This behavior is consistent with the diffusion residence time model of Hadgu *et al.*[32]

In a previous study, in addition to $m_{o\,exp}$ values, the $m_{o\,cal}$ data were also calculated for conventional THGAs,[33] yielding $m_{o\,cal}/m_{o\,exp}$ ratios of 0.79 for As and 0.73 for Se under interrupted internal furnace gas flow during atomization and Zeeman effect BG correction.[33] These ratios point to slightly lower atomization efficiency for Se in standard THGA tubes. The current $m_{o\,cal}$ data for As and Se in end-capped THGAs were calculated to be 19 pg and 27 pg, respectively, giving $m_{o\,cal}/m_{o\,exp}$ ratios of 0.86 and 0.75 – slightly higher than those observed for conventional THGA tubes.[33] These results suggest a bit greater atomization efficacy of As and Se in end-capped tubes, possibly owing to the more favorable axial temperature distribution and lower analyte loss at the tapered tube ends, consistent with earlier observations on end-capped THGAs.[32] Higher efficiency could be attained by decreasing the mass of Mg, whose excess likely increases the background noise, and consequently the blank value.

Method validation and sample analysis. The mean recoveries obtained were 93.1 ±13.7% for As and 93.1 ±9.2% for Se (Table 7). The estimated dry matrix residue for the studied samples, obtained after the graphite furnace drying steps ranged from 0.09 to 0.60 mg

Table 7. Recovery and precision for fruit juice samples spiked with 50 µg/L of As and Se

Sample	Estimated dry matrix Residue (mg/5 µL)	Element			
		As		As	
		Recovery %	RSD %	Recovery %	RSD %
Peach juice	0.45	89.2	0.8	90.9	6.6
Apple juice	0.55	87.4	3.4	101.2	3.3
Mixed (Carrot, Apple, Raspberry)	0.44	80.3	0.6	83.1	4.2
Grape juice	0.40	85.7	2.9	65.9	6.5
Peach juice	0.40	89.6	2.9	95.5	4.1
Orange juice	0.40	77.7	9.6	96.9	6.1
Apple juice	0.39	105.4	1.9	98.7	5.9
Grape juice	0.09	111.7	4.2	96.0	2.4
Apple juice	0.55	111.9	1.8	104.1	0.2
Mixed (Carrot, Apple, Peach)	0.44	68.0	0.9	83.7	4.9
Mixed – Red fruits	0.60	82.4	3.1	96.5	0.5
Apple juice	0.40	93.2	3.6	97.4	6.6
Peach juice	0.09	94.9	4.6	91.4	2.3
Apple juice	0.55	88.9	0.5	94.8	0.1
Apple juice	0.09	111.6	0.9	94.7	2.5
Orange juice	0.09	111.8	2.2	99.6	1.7
Mean	0.37	93.1 ± 13.7	2.7 ± 2.3	93.1 ± 9.2	3.6 ± 2.3

Abbreviations: RSD – relative standard deviation.
Estimated dry matrix residue was calculated for fruit juice samples based on labeled sugar content (assumed to represent the dominant fraction of total soluble solids).

per 5 µL sample. Linear regression analysis revealed a significant negative relationship between matrix residue and As recovery (R^2=30.7%, p=0.026), indicating that increasing matrix load reduced recovery (Fig. S3a). In contrast, no significant correlation was observed for Se recovery (R^2=0.0%, p=1.000), suggesting that Se determination was not affected by the evaluated range of matrix residue (Fig. S3b). However, despite the trend of As, satisfactory mean recoveries were obtained for both elements across all measured fruit juice samples, demonstrating adequate accuracy for routine analysis. The slightly broader recovery ranges obtained for some samples may reflect compositional difference among fruit juices – particularly variations in sugar, acid, and additive content – which can affect modifier performance, and consequently the atomization efficiency and background absorption. The similar average recovery observed for As and Se indicates that both elements underwent comparable stabilization under the present graphite furnace conditions. The precision of the method expressed as the average RSD, was 2.7% ± 2.3% for As and 3.6% ±2.3% for Se, confirming good repeatability of the replicate determinations (<5%). For CRM analysis (TMDA-51), recoveries of 107% and 105% were obtained for As and Se, respectively.

Oliveira *et al.*[55] reported a direct sampling GFAAS method to determine Se in fruit juices, using As as an internal standard and permanent modifiers – tungsten/rhodium carbide coating or tungsten coating with Pd – on the graphite atomizer surface. The method achieved lower LODs (0.35-0.7 µg/L). Without the internal standard, recoveries were lower (77-89%), whereas applying the internal standard to correct for signal drift improved recovery to 98-102%. In the present study, the simultaneous determination of As and Se was achieved without permanent tube coating or internal standardization, but using a Pd–Mg modifier that provided efficient thermal stabilization of both analytes. Although the current LODs are slightly higher, the method offers notable advantages in cost efficiency, operational simplicity, and analytical throughput, making it a practical and sustainable alternative for routine fruit juice screening. The As and Se concentrations in all analyzed fruit juice samples were below the LOD and are therefore considered safe, as they are below the recommended maximum allowable limits.

Greenness assessment. The AGREE score of 0.65 (Fig. 6) indicates good compliance with the principles of green analytical chemistry. This favourable score was mainly attributed to direct sample analysis without off-line sample preparation, low sample and reagent consumption, absence of derivatization, low analytical waste generation, and simultaneous determination of As and Se in a single atomization cycle. Lower scores were mainly associated with the inability to perform in situ measurements, the use of non-renewable and hazardous reagents (*e.g.*, nitric acid and hydrogen peroxide) and energy consumption inherent to GFAAS utilizing electrothermal heating. Nevertheless, the developed method substantially reduced reagent consumption, waste generation, and analysis time compared with conventional digestion-based methods, thereby demonstrating improved environmental sustainability.

Risk assessment. In line with EFSA's updated approach[4] risk was contextualized using the $BMDL_{05}$ for iAs (0.06 µg/kg body weight/day) and the margin-of-exposure (MOE) concept.

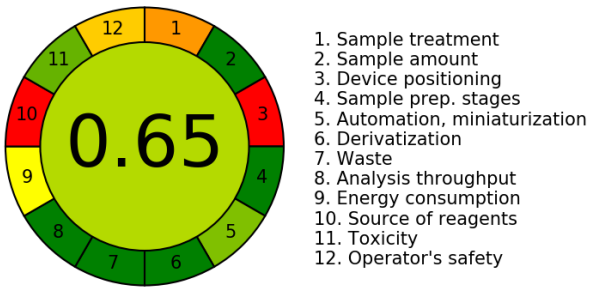

Fig. 6 Chart of greenness assessment performed with AGREE software on the developed direct sampling GFAAS method.

$$MOE = \frac{Reference\ point_{BMDL\ 05}}{Exposure} \quad (4)$$

Although As was not detected in any sample (C_{As} <LOD of 2.1 µg/L), a conservative upper-bound (UB) scenario was applied using the LOD as the assumed As concentration in accordance with EFSA guidance on left-censored data. The estimated daily intake (EDI) was calculated based on an average juice consumption of 0.150 L/day for a 70 kg adult,[56] yielding a UB exposure of 0.005 µg/kg body weight per day and an MOE of 12 relative to EFSA reference point[4] – derived to cover multiple health endpoints, including cancer and other chronic diseases associated with long-term iAs exposure.

All fruit juice samples showed Se concentrations below the LOD (2.5 µg/L); therefore, no detailed risk assessment was required. To confirm the absence of risk, a conservative UB exposure was estimated by setting the Se concentration to the LOD. The resulting EDI of 0.005 µg/kg body weight per day was less than 0.2% of EFSA's adult tolerable upper intake level (calculated, 3.64 µg/kg/body weight, from 255 µg/day for a 70 kg adult)[48]. The potential exposure from fruit juice consumption was therefore negligible and well below any level of toxicological concern.

CONCLUSION

In this study, a digestion-free, simultaneous GFAAS method was developed for routine analysis of total As and Se in fruit juices. The SIMAA 6000 spectrometer, equipped with an end-capped THGA tube furnace, longitudinal Zeeman effect background correction, operated under optimized graphite furnace heating program (pyrolysis: 1300 °C; atomization: 2100 °C), and using Pd–Mg chemical modifier and oxidizing reagent (H_2O_2+HNO_3), enabled reliable simultaneous analysis of both analytes. An optimum sample volume of 5 µL was identified; increasing the volume above this progressively reduced the analyte recovery. Among the assessed interferents, phosphate exhibited the strongest suppressive effect, while chloride and sulfate caused only minor interference under optimized conditions. The method demonstrated satisfactory sensitivity, precision, and accuracy with excellent linearity up to 150 µg/L for both As and Se. Arsenic and Se levels in all sixteen commercial fruit juice samples were below the respective LODs. The theoretical characteristic masses of As and Se for end-capped THGAs obtained from model calculations were in good agreement with the corresponding experimental data of the developed method, highlighting the value of theoretical sensitivity calculations in validating novel GFAAS methods. A conservative exposure assessment indicated no toxicological risk for either element.

Overall, the developed method is a rapid, simple, and sustainable analytical approach requiring only microliter sample and reagent volumes without sample digestion. It provides reliable single-cycle simultaneous analysis of As and Se, suitable for routine monitoring. Although ICP-MS offers higher sensitivity for element quantitation at ng/L levels, the proposed GFAAS method offers cost-effective, green analytical alternative with acceptable sensitivity for fruit juice screening. Additionally, it can be readily implemented to HR-CS-GFAAS technology.

ASSOCIATED CONTENT

The supporting information (Tables S1 and Figs. S1−S3) is available at https://www.at-spectrosc.com

AUTHOR INFORMATION

Zsolt Ajtony received his PhD in Chemistry from Eötvös Loránd University in 1989. He is an associate professor in the Food Science Department at Széchenyi István University. His research focuses on analytical chemistry, including Mass Spectrometry, Chromatographic techniques (HPLC and GC), Spectroscopic methods such as GFAAS, with emphasis on the development and validation of analytical methods for chemical analysis. He has extensive experience in laboratory management, quality assurance, and the accreditation of analytical laboratories in accordance with international standards. He has published over 50 scientific papers and has an h-index of 16 and an i10-index of 26.

Corresponding Author

* Z. Ajtony

Email address: ajtony.zsolt@ga.sze.hu

Notes

The authors declare no competing financial interest.

REFERENCES

1. A. Szymczycha-Madeja, M. Welna, D. Jedryczko, and P. Pohl, *TrAC Trends Anal. Chem*., 2014, **55**, 68–80. https://doi.org/10.1016/j.trac.2013.12.005
2. ATSDR. Substance Priority List, U.S. Department of Health and Human Services, CDC, 2026. https://www.atsdr.cdc.gov/programs/substance-priority-list.html
3. FDA. Closer to Zero: Reducing Childhood Exposure to Contaminants from Foods, 2024. https://www.fda.gov/food/environmental-contaminants-food/closer-zero-reducing-childhood-exposure-contaminants-foods
4. EFSA Panel on Contaminants in the Food Chain, *EFSA J*., 2024, **22**, e8488. https://doi.org/10.2903/j.efsa.2024.8488
5. European Food Safety Authority, D. Arcella, C. Cascio, and J. Á. Gómez Ruiz, *EFSA J*., 2021, **19**, e06380. https://doi.org/10.2903/j.efsa.2021.6380
6. M. H. Al Amin, C. Xiong, K. A. Francesconi, Y. Itahashi, M. Yoneda, and J. Yoshinaga, *Chemosphere*, 2020, **239**,124781. https://doi.org/10.1016/j.chemosphere.2019.124781
7. Z. Ajtony, N. Szoboszlai, Zs. Bella, Sz. Bolla, P. Szakál, and L. Bencs, *Microchim. Acta*, 2005, **150**, 1–8. https://doi.org/10.1007/s00604-005-0330-y
8. M. Naderi, P. Puar, M. Zonouzi-Marand, D. P. Chivers, S. Niyogi, and R. W. M. Kwong, *Sci. Total Environ.*, 2021, **767**, 144329. https://doi.org/10.1016/j.scitotenv.2020.144329
9. B. Sadee B, M. E. Foulkes, and S. J. Hill. *J. Anal. At. Spectrom.*, 2015, **30**, 102-218. http://dx.doi.org/10.1039/C4JA00269E
10. A. Dehelean, and D. A. Magdas, *Sci. World J.*, 2013, **1**, 1-6. https://dx.doi.org/10.1155/2013/215423
11. M. Anastácio, A. P. M. dos Santos, M. Aschner, and L. Mateus. *Toxicol. Rep.*, 2018, **5**, 434-439. https://www.sciencedirect.com/science/article/pii/S2214750018300076
12. G. Chen and B. Lai, *Anal. Bioanal. Chem.*, 2024, **416**, 839–847. https://dx.doi.org/10.1007/s00216-023-05071-1
13. S. D. Conklin and P. E. Chen, *Food Addit. Contam. A*, 2012, **29**, 1272-1279. https://doi.org/10.1080/19440049.2012.687775
14. K. Ljung, B. Palm, M. Grandér,and M. Vahter, *Food chem.*, 2011, **127**, 943-951. https://doi.org/10.1016/j.foodchem.2011.01.062
15. P. Shavali Gilani, P. Sadighara, S. N. Vakili, N. Yazdanfar , and M. Yousefi, *J. Agric. Food Res.*, 2025, **21**, 102014. https://doi.org/10.1016/j.jafr.2025.102014
16. S. X. Bao, Z. H. Wang, and J. S. Liu, *Spectrochim. Acta B.*, 1999, **54**,1893-1897. https://doi.org/10.1016/S0584-8547(99)00160-3
17. I. J. Cindrić, M. Zeiner, M. Kröppl, and G. Stingeder, *Microchem. J.*, 2011, **99**, 364–369. https://doi.org/10.1016/j.microc.2011.06.007
18. R. E. S. Froes, W. B. Neto, N. O. C. Silva, R. L. P. Naveira, C. C. Nascentes, and J. B. B. da Silva, *Spectrochim. Acta B*, 2009, **64**, 619–622. https://doi.org/10.1016/j.sab.2009.06.006
19. M. Gorska and P. Pohl, *J. Anal. At. Spectrom.*, 2021, **36**, 1455–1465. https://doi.org/10.1039/d1ja00127b
20. P. Pohl, A. Dzimitrowicz, P. Jamroz, and K. Greda, *Microchem. J.*, 2018, **140**, 248–255. https://doi.org/10.1016/j.microc.2018.04.032
21. I. N. Pasias, N. I. Rousis, A. K. Psoma, and N. S. Thomaidis, *Atom. Spectrosc.*, 2021, **42**, 310-327. https://doi.org/10.46770/as.2021.707
22. J. M. Harnly, *Fresenius J. Anal. Chem.*, 1996, **355**, 501–509. https://doi.org/10.1007/s0021663550501
23. B. G. Beltrán, V. Ramos-Sanchez, D. Chávez-Flores, R. Rodríguez-Maese, and E. Palacio, *J. Chem.*, 2020, 1–9. https://doi.org/10.1155/2020/8817393
24. P. Pohl, P. Jamroz, K. Greda, M. Gorska, A. Dzimitrowicz, M. Welna, and A. Szymczycha-Madeja, *Anal. Chim. Acta*, 2021, **1169**, 338399. https://doi.org/10.1016/j.aca.2021.338399
25. L. Fernández-López, B. Gómez-Nieto, M. J. Gismera, M. T. Sevilla, and J. R. Procopio, *Spectrochim. Acta B*, 2018, **147**, 21–27. https://doi.org/10.1016/j.sab.2018.05.016
26. M. Ibourki, O. Hallouch, K. Devkota, D. Guillaume, A. Hirich, and S. Gharby, *J. Food Compos. Anal.*, 2023, **120,** 105330. https://doi.org/10.1016/j.jfca.2023.105330
27. B. V. L'vov, Talanta, 1976, **23**, 109–118. https://doi.org/10.1016/0039-9140(76)80032-X
28. W. Slavin and G. R. Carnrick, *Spectrochim. Acta B*, 1984, **39**, 271–282. https://doi.org/10.1016/0584-8547(84)80035-X
29. B. Welz and M. Sperling, Atomic Absorption Spectrometry, 3rd ed., Wiley-VCH, 1999. https://doi.org/10.1002/9783527611690
30. B. V. L'vov, V.G. Nikolaev, E.A. Norman, L.K. Polzik, and M. Mojica, *Spectrochim. Acta B*, 1986, **41**, 1043–1053. https://doi.org/10.1016/0584-8547(86)80125-2
31. B. V. L'vov, *Spectrochim. Acta B*, 1990, **45**, 633–655. https://doi.org/10.1016/0584-8547(90)80046-L
32. N. Hadgu, K. E. A. Ohlsson, and W. Frech, *Spectrochim. Acta B*, 1996, **51**, 1081–1093. https://doi.org/10.1016/0584-8547(96)01463-2.
33. L. Bencs, N. Laczai, and Z. Ajtony, *Spectrochim. Acta B*, 2015, **109**, 52–59. https://doi.org/10.1016/j.sab.2015.05.001.
34. L. Bencs, *Can. J. Anal. Sci. Spect.*, 2008, **53**, 52-58. https://www.researchgate.net/publication/237713336
35. F. Pena-Pereira, W. Wojnowski, and M. Tobiszewski, *Anal. Chem.*, 2020, **92**, 10076-10082. https://doi.org/10.1021/acs.analchem.0c01887
36. Z. Ajtony, N. Szoboszlai, E. K. Suskó, P. Mezei, K. György, and L. Bencs, *Talanta*, 2008, **76**, 627-634. https://doi.org/10.1016/j.talanta.2008.04.014
37. A. B. Volynsky, *Spectrochim. Acta B*, 2000, **55**, 103–150. https://doi.org/10.1016/S0584-8547(99)00175-5.
38. E. Bulska and H. M. Ortner, *Spectrochim. Acta B*, 2000, **55**, 491–499. https://doi.org/10.1016/S0584-8547(00)00201-9
39. H. M. Ortner, E. Bulska, U. Rohr, G. Schlemmer, S. Weinbruch, and B. Welz, *Spectrochim. Acta B*, 2002, **57**, 1835–1853. https://doi.org/10.1016/S0584-8547(02)00140-4
40. S. Vinter, J. Filip, J. Sotolarova, B. Tomaskova, J. Reznicek, and P. Jerabek, *Talanta*, 2026, **299**, 129125. https://doi.org/10.1016/j.talanta.2025.129125
41. C. S. Dakuzaku, G. P. G. Freschi, M. de Moraes, J. A. Nóbrega, and J. A. Gomes Neto, *Atom. Spectrosc.*, 2001, **22**, 271–278. https://www.at-spectrosc.com/as/article/abstract/200102001
42. D. L. Tsalev, T. A. Dimitrov, and P. B. Mandjukov, *J. Anal. At. Spectrom.*, 1990, **5**, 189–194. https://doi.org/10.1039/JA9900500189
43. M. A. Z. Arruda, M. Gallego, and M. Valcárcel, *J. Anal. At. Spectrom.*, 1994, **9**, 657–662. https://doi.org/10.1039/JA9940900657
44. R. W. B. Pearse and A. G. Gaydon, The Identification of Molecular Spectra, 3rd ed., Chapman & Hall, London, 1963. https://doi.org/10.1016/0010-2180(64)90042-2
45. B. Welz, H. Becker-Ross, S. Florek, and U. Heitmann, High-Resolution Continuum Source AAS: The Better Way to Do Atomic Absorption Spectrometry, Wiley-VCH, VerlagGmbH & Co. KgaA,

Weinheim, Germany, 2005; pp. 62–63. https://doi.org/10.1002/3527606513

46. B. Radziuk and Y. Thomassen, *J. Anal. At. Spectrom.*, 1992, **7**, 397–403. https://doi.org/10.1039/JA9920700397
47. J. Y. Cabon and A. Le Bihan, *Anal. Chim. Acta*, 1999, **402**, 327–338. https://doi.org/10.1016/S0003-2670(99)00501-2.
48. I. Martinsen, B. Radziuk, and Y. Thomassen, *J. Anal. At. Spectrom.*, 1988, **3**, 1013–1022. https://doi.org/10.1039/JA9880301013
49. A. Kramida YR, J. Reader, and NIST ASD Team. NIST Atomic Spectra Database. 2026. https://doi.org/10.18434/T4W30F
50. M. J. B. de Souza, M. C. Barciela-Alonso, M. Aboal-Somoza, and P. Bermejo-Barrera, *Braz. J. Anal. Chem.*, 2022, **9**, 49–61. htttp:/doi.org/10.30744/brjac.2179-3425.AR-87-2021
51. EFSA Panel on Nutrition. *EFSA J.*, 2021, **21**, e07704. https://doi.org/10.2903/j.efsa.2023.7704
52. Z. Ajtony, N. Laczai, N. Szoboszlai, and L. Bencs, *Atom. Spectrosc.*, 2014, **35**, 33–42. https://doi.org/10.46770/AS.2014.01.005
53. J. Michon, V. Deluchat, R. Al Shukry, C. Dagot, and J. C. Bollinger, *Talanta*, 2007, **71**, 479–485. https://doi.org/10.1016/j.talanta.2006.06.016.
54. L. Bezúr, *Microchem. J.*, 1998, **59**, 107–116. htttp:/doi.org/10.1006/mchj.1998.1569
55. A. P. Oliveira, J. A. G. Neto, J. A. Nóbrega, P. R. M. Correia, and P. V. Oliveira, *Food Chem.*, 2005, **93**, 355–360. htttp:/doi.org/10.1016/j.foodchem.2004.11.024
56. J. Walton and L. Kehoe, *Nutr. Res. Rev.*, 2025, **38**, 69–80. https://doi.org/10.1017/S095442242400009X